Radiation protection of patients: status of primary standard dosimetry of high-energy photon and electron beams in Austria

Baumgartner Andreas[1]; Steurer Andreas[2]; Maringer Franz Josef[2]

[1]University of Natural Resources and Life Sciences Vienna, LLC-Laboratory Arsenal, Faradaygasse 3, Arsenal 214, 1030 Vienna, Austria
[2]BEV - Bundesamt für Eich- und Vermessungswesen (Federal Office of Metrology and Surveying), Arltgasse 35, 1160 Vienna, Austria

Abstract. In Austria, a Domen-type absorbed dose graphite calorimeter is used to realize the unit of absorbed dose to water. It was developed by the National Metrology Institute of Austria (BEV) in cooperation with the Research Centers Seibersdorf. The graphite calorimeter is designed for quasi-adiabatic and quasi-isothermal mode of operation. The absorbed dose conversion is done by two methods based on the photon-fluence scaling theorem. The graphite calorimeter was originally designated for determination of absorbed dose to water in ^{60}Co beams. The progress in radiation therapy required the development of the graphite calorimeter to enable primary standard dosimetry of high-energy photon and electron beams. Therefore a set of beam quality dependent conversion and correction factors was required. They were mainly obtained via Monte Carlo simulations with PENELOPE code and measurements. The determination of correction factors for ^{60}Co beams led to the re-evaluation of the absorbed dose rate to water reference value for ^{60}Co beams. For validation the BEV participated in the international key comparison for absorbed dose to water in ^{60}Co gamma radiation at the BIPM. To achieve beam quality specific correction factors it was necessary to consider the beam characteristics of irradiation facilities. This included Monte Carlo modelling of the BEV ^{60}Co therapy unit and of Varian Linac treatment heads. The determined photon energy spectra constitute the basis of beam models used for Monte Carlo simulations to obtain the required correction factors. Further concepts were developed for primary standard dosimetry of high-energy electron beams. A confirmation of the graphite calorimeter development and respectively of the implemented correction and conversion factors was done in the framework of an EURAMET project - intended for the direct comparison of absorbed dose primary standards in ^{60}Co and high-energy photon beams. The advance of the graphite calorimeter provides the methodical fundamentals to enable the BEV for the accomplishment of primary standard dosimetry of high-energy photon and electron beams. The improvement of the primary standard directly leads to an improvement of quality assurance measurements in Linac radiotherapy, i.e. directly related to the radiation protection of patient. Since the accurate knowledge of the applied dose is a main factor influencing the success of a radiotherapy and therefore of great importance for the treatment planning.

Key Words: primary standard dosimetry; absorbed dose; graphite calorimeter; Monte Carlo

1. Introduction

A primary standard absorbed dose graphite calorimeter is used to realize the unit of absorbed dose to water at the Federal Office of Metrology and Surveying (BEV - Bundesamt für Eich- und Vermessungswesen) which is the National Metrology Institute (NMI) and national authority on legal metrology in Austria. The graphite calorimeter is a Domen-type calorimeter and is in operation since 1983. A detailed description of the graphite calorimeter components, operation/calibration modes can be found in [1],[2]. A review on photon absorbed dose standards used by other NMI's is given in [3]. The graphite calorimeter was originally designated for determination of absorbed dose to water in ^{60}Co gamma ray beams. The progress in radiation therapy within the recent years forced increased demands on high-energy photon dosimetry (i.e. photons generated with accelerators). To meet the needs the application range of the primary standard was extended, to enable measurements at medical accelerators and ionization chamber calibrations in terms of absorbed dose to water at high-energy photon beams. To conduct the energy range and application enhancement a set of beam quality dependent conversion and correction factors was required. Additionally the graphite calorimeter, the graphite phantom and all corresponding components had to be adapted to the measurement requirements for high-energy photon beams. This was done within a refurbishment and modernization process intended to ensure the quality and reliability of the primary standard, see [4].

The measurement capacities of the BEV regarding irradiation facilities for photon therapy are limited to a Picker C8M/80 ^{60}Co teletherapy unit. To perform measurements at high-energy photon beams the BEV entered into collaboration with the Wiener Neustadt hospital. The hospital operates the Varian linear accelerators types Clinac 2100C and 2300C/D (nominal accelerator potentials: 4 MV, 6 MV, 10 MV and 15 MV for the generation of photon beams).

The accomplishment of the energy range and application enhancement of the graphite calorimeter was executed in a stepwise manner. First of all measurements and simulation studies for the estimation of correction factors were carried out for ^{60}Co gamma rays to achieve a well-founded basis, see [4]. This lead to the re-evaluation of the BEV absorbed dose rate to water reference value for ^{60}Co gamma ray beams.

For validation the BEV participated in the international key comparison (BIPM.RI(I)-K4 key comparison) for the absorbed dose to water in ^{60}Co gamma radiation at the Bureau International des Poids et Mesures (BIPM) in March 2009 [5]; thereby a calibration coefficient ratio of 0.9996 of the BEV and the BIPM standards for the absorbed dose to water was achieved.

Subsequently measurements and Monte Carlo studies for selected high-energy photon beam qualities were performed. This paper presents the status of primary standard dosimetry of high-energy photon and electron beams in Austria; due to a conducted enhancement of the working and application range of the BEV graphite calorimeter; based upon the determined beam quality specific correction and conversion factors. The verification of those factors was done within the EURAMET Project 1021 [4],[6],[7].

2. Materials and methods

The reference conditions for the realization of the unit of absorbed dose to water, in high-energy photon beams, are taken according to [1],[8],[9],[10],[11]. The distance from the source to the center of the detector is 110 cm. The field size in air is 10×10 cm² at a source to surface distance (SSD) of 100 cm to the water phantom. The reference depth in the water phantom is 10 g cm^{-2}. The reference conditions for the measurements with the graphite calorimeter and the ionization chamber in the graphite phantom result from application of the photon-fluence scaling theorem for Compton-scattered radiation [12]. The scaling factor SF = 1.572 is used to obtain the required scaled reference distance, field size and measuring depth. SF is defined as the ratio of the distance in water and the scaled distance in graphite.

2.1. Determination of absorbed dose to graphite

Absorbed dose to graphite (D_g) measurements at high-energy photon beams are be performed in the quasi-adiabatic operation mode [2] of the graphite calorimeter. The evaluation of the measurements is done according to equation (1).

$$D_{\mathrm{g,adiabat.}} = c_p \cdot \Delta T_{\mathrm{c}} = \frac{1}{m_{\mathrm{c}}} \cdot K_{\mathrm{ad}} \cdot k_1 \cdot k_{\mathrm{gap}} \cdot k_{\mathrm{gc}} \cdot k_{bu} \qquad \text{with} \qquad K_{\mathrm{ad}} = \left(\frac{\Delta R}{R} + k_2 \cdot \Delta U \right) \tag{1}$$

The energy imparted to the core with mass m_c and specific heat capacity c_p causes a temperature rise within the core ΔT_c. The heat defect of graphite is neglected, as declared in [3],[9]. D_g is determined by evaluating the change in resistance of the core thermistors $\Delta R/R$ and the temperature drift correction $k_2 \cdot \Delta U$; these terms are summarized as the correction factor for quasi-adiabatic operation K_{ad}. The factor k_2 is the chart calibration factor and ΔU is the difference in voltage. The temperature dependent quasi-adiabatic calibration factor k_1 is taken from a linear fit within the graphite calorimeter electrical calibration curve considering the actual temperature working point. Further the correction for the effect of the gaps k_{gap} and the correction for the effective graphite calorimeter measurement depth k_{gc} are taken into account by the determination of D_g. The correction for the beam non-uniformity k_{bu} is taken as unity and only considered within the uncertainty budget based on the results of the investigations in [13].
For the evaluation of the measurements and electrical calibrations a LabVIEW based evaluation program is used. The program provides automatic non-linear temperature drift extrapolations.

2.2. Absorbed dose conversion

The conversion from absorbed dose to graphite to absorbed dose to water D_w is done by two methods: by calculation according to equation (3) based upon equation (2) and experimental by ionization chamber measurements in the water phantom and the graphite phantom according to equation (4). The fist method uses the ratio of the collision kerma described by $\Psi \cdot (\overline{\mu_{en}} / \rho)$. Ψ is the photon energy fluence, $(\overline{\mu_{en}} / \rho)_{w,g}$ is the ratio of the average mass-energy absorption coefficients and β is the ratio of the absorbed dose to collision kerma.

$$D_{\mathrm{w}} = D_{\mathrm{g}} \cdot \left(\frac{\Psi_{\mathrm{w}}}{\Psi_{\mathrm{g}}} \right) \cdot \left(\frac{\overline{\mu_{\mathrm{en}}}}{\rho} \right)_{\mathrm{w,g}} \cdot \beta_{\mathrm{w,g}} \tag{2}$$

The conversion procedures are based on the photon-fluence scaling theorem [12]. Thus all source to reference point distances, measuring depths, the phantom size and the field size are scaled in the inverse ratio of the electron densities of water and graphite. This ensures that the energy spectra of the primary and scattered photons and their distribution in angle at the corresponding scaled points of measurement will be the same. Consequently the photon energy fluence ratio equals the inverse square of the distances from the source to the corresponding measuring points R_g and R_w, see equation (3).

$$D_{\mathrm{w}} = D_{\mathrm{g}} \cdot \left(\frac{R_{\mathrm{g}}}{R_{\mathrm{w}}} \right)^2 \cdot \left(\frac{\overline{\mu_{\mathrm{en}}}}{\rho} \right)_{\mathrm{w,g}} \cdot \beta_{\mathrm{w,g}} \cdot k_{\Delta\mathrm{air}} \cdot k_{\mathrm{gs}} \cdot k_{\mathrm{depth}} \cdot k_{\mathrm{front}} \cdot k_{\mathrm{bs}} \cdot k_{\mathrm{pp}} \text{ (Method 1)} \tag{3}$$

The corrections applied in equation (3) are: the correction factor $k_{\Delta air}$ for the difference in air attenuation, the scaling correction $k_{gs,}$ the correction factor k_{depth} to consider the depths in graphite and in water, k_{front} to consider when appropriate the front wall of the water phantom, the bremsstrahlung and annihilation radiation correction k_{bs} and the pair production correction k_{pp}. According to investigations of [14] the correction k_{bs} was assumed to be unity and is only considered within the uncertainty budget. The numerical value for the correction k_{pp} was taken as unity and its uncertainty was estimated based upon the numerical values of the corrections calculated in [14]. For the corrections k_{depth} and k_{front} the value unity is assumed and they are considered within the uncertainty budget. The conversion method 1 relies on the accurate knowledge of the virtual point source position. In general the estimation of its location can be done experimentally throughout ionization chamber measurements in air along the beam axis or by Monte Carlo simulations or with a combination of both. Since it is intended by the BEV to perform measurements at various accelerators the virtual source location has to be estimated for each beam quality. Therefore the virtual source position is estimated based upon ionization chamber measurements, according to [15] or in combination of measurements with a simple method for calculating the position using the geometry of the flattening filter [16].
The experimental dose conversion method uses an ionization chamber as transfer instrument. Thereby a thin walled PTW ionization chamber type 30012 is used. The collected charge in graphite Q_g and the collected charge in water Q_w (both corrected for air density, air humidity and saturation according to [11]) are measured to perform the absorbed dose conversion according to equation (4).

$$D_w = D_g \cdot \frac{Q_w \cdot s_{w,air} \cdot p_{Q,w} \cdot k_{depth} \cdot k_{front}}{Q_g \cdot s_{g,air} \cdot p_{Q,g} \cdot k_{gi}} \quad \text{(Method 2)} \qquad \text{with } p_Q = p_{wall} \cdot p_{cav} \cdot p_{dis} \cdot p_{cel} \quad (4)$$

Here, $s_{w,air}$ and $s_{g,air}$ are the restricted collision mass stopping power ratios of water to air and graphite to air, derived from [1]. The chamber perturbation correction factors in water $p_{Q,w}$ and graphite $p_{Q,g}$ respectively are defined as product of the wall correction factor p_{wall}, fluence correction factor p_{cav}, displacement correction factor p_{dis} and the central electrode correction factor p_{cel}. The correction p_{cel} was assumed to be equal for the chamber in the graphite- and water phantom. The factor k_{gi} corrects for the effective ionization chamber measuring depth in the graphite-phantom. The correction factor k_{depth} considers in the case of ionization chamber measurements the chamber position in graphite and in water. The value unity was assumed for k_{depth} and further considered in the uncertainty budget. It should be mentioned that in the case of measurements at ^{60}Co gamma ray beams the thick walled CC01 ionization chamber is used by applying the cavity theory [1].

2.3. Monte Carlo beam models

For the determination of the required graphite calorimeter correction factors the Monte Carlo code system PENELOPE-2006 [18] was used. The code allows the calculation of coupled electron-photon transport in various materials from a few hundred eV to about 1 GeV.

To achieve beam quality specific correction factors it was necessary to consider the radiation field characteristics of irradiation facilities used for measurements. This included the Monte Carlo modelling of Varian Linac treatment heads with the use of PENELOPE penmain code. Thereby photon energy spectra were determined. The spectral photon fluence was scored at two distances: one distance equal to a SSD of 100 cm and one with about 64 cm SSD which corresponds to the scaled SSD used for the graphite calorimeter measurements. The defined scoring planes had cross sections of 10×10 cm² and 6.4×6.4 cm², respectively. These spectra constitute the basis of beam models used for the graphite calorimeter specific Monte Carlo simulations to obtain the required correction factors. The determination and verification of these beam models is presented in [19]. Altogether five beam models of high-energy photon beams from Varian Linacs were used for the determination of the gap effect correction, the correction for the difference in air attenuation and the scaling correction. Thereby the 4 MV, 6MV, 10 MV and 15MV photon beams were considered. Additionally a photon beam model calculated with the 10 MV treatment head and 11 MeV electrons was used. Further a 25 MV beam model with the photon energy spectrum of an Elekta SL25 accelerator published in [20] was implemented.

2.4. Description and determination of the graphite calorimeter correction factors

The required beam quality specific corrections for the graphite calorimeter were obtained via Monte Carlo simulations and measurements, with the graphite calorimeter itself, and ionization chambers. A major component from the set of correction factors applied to the graphite calorimeter is the correction for the effect of the gaps k_{gap}, see [21],[22]. The correction factor accounts for the beam perturbation caused by the air gap and the vacuum gaps around the core and the surrounding graphite calorimeter bodies. This correction was determined by Monte Carlo simulations using two geometry models (with and without gaps), according to [21],[22]. In the case of the model without gaps these gaps were filled with graphite. To compensate for this the thickness of the graphite plates in front of the graphite calorimeter core was reduced to ensure that the depth of graphite from the phantom surface to the middle of the core remains the same. For the simulations the electron and positron transport was not considered within the back scatter plate of the graphite phantom. In the other parts of the graphite calorimeter models photon interactions were simulated until their energies fell below 10 keV. Electron and positron interactions were simulated for particle energies exceeding 100 keV. The cut-off energy loss for hard inelastic collisions W_{cc} was set to 10 keV and the cut-off W_{cr} for hard bremsstrahlung emission was set to 5 keV. In this manner about 5×10^9 initial photon histories were simulated.

The scaling correction k_{gs} accounts for the deviation of the graphite phantom dimensions, both in size and shape, from the exact scaling requirements. For the determination of the scaling correction a cylindrical geometry model according to the real graphite calorimeter phantom and one exactly scaled graphite cube was used. They consist of one material and two bodies. These bodies are the core -

where the energy deposited is scored - and the surrounding cylindrical or cubic phantom. The simulation parameters were set to neglect electron and positron transport. Photon interactions were simulated for energies exceeding 1 keV. In that way about 5×10^{10} initial photon histories were simulated.

The correction factor $k_{\Delta air}$ accounts for the difference in air attenuation at the corresponding measurement distances as a result of the application of the photon-fluence scaling theorem. For its determination the photon energy fluence was scored at one distance equal to the SSD of the water phantom, and at the corresponding scaled SSD of the graphite phantom. The usage of tabulated attenuation coefficients for air taken from [23] allowed the calculation of mean attenuation coefficients $\overline{\mu}/\rho$ for the simulated spectra at the reference distances. With these mean attenuation coefficients the air attenuation correction factors $k_{\Delta air}$ were estimated according to equation (5).

$$k_{\Delta air} = \frac{e^{-\frac{\overline{\mu}}{\rho}\cdot\rho_{air}\cdot R_w}}{e^{-\frac{\overline{\mu}}{\rho}\cdot\rho_{air}\cdot R_g}} \qquad \text{with} \qquad \frac{\overline{\mu}}{\rho} = \frac{\int_0^{E_{max}} \Psi(E)\cdot\frac{\mu(E)}{\rho}\cdot dE}{\int_0^{E_{max}} \Psi(E)\cdot dE} \tag{5}$$

Here, ρ_{air} air is the density of air, $\Psi(E)$ is the differential photon energy fluence at the defined scoring planes and $\mu(E)/\rho$ are the mass attenuation coefficients of air for photons of energy E. In the case of the 25 MV spectrum from the Elekta SL 25 only a spectrum at one distance was available. Thus the calculation neglects the difference in the mean mass attenuation coefficients at the corresponding distances.

The corrections for the effective measurement depths in graphite k_{gc} and k_{gi} account for the required measuring depth of 11.111 g cm^{-2} in graphite. This depth cannot be realized exactly with the graphite phantom. The effective graphite calorimeter measuring depth is 10.495 g/cm². In the case of ionization chamber measurements in the graphite phantom an effective measuring depth of 10.565 g/cm² can be realized.

2.5. Concepts for the primary standard dosimetry of high-energy electron beams with BEV graphite calorimeter

For measurements in high-energy electron beams concepts were developed for the implementation of a primary standard dosimetry with the graphite calorimeter, see [6]. The practical implementation still requires adaptations of the graphite phantom at the metrological requirements of those radiation fields.

3. Results and discussion

Within this paper the tissue phantom ratio ($TPR_{20,10}$) is utilized as beam quality index to characterize the high-energy photon beams, see [8],[9],[10],[11]. The Monte Carlo calculated correction factors were evaluated for the application range of the graphite calorimeter as a function of $TPR_{20,10}$ to be independent of a special Linac. A similar method was applied to the conversion factors which were taken from literature.

3.1. Beam quality specific correction factors

The beam quality specific corrections for the graphite calorimeter were determined by Monte Carlo simulations with use of Linac photon energy spectra. Figure 1 displays the results of the simulations with their statistical standard uncertainties. By this means the results of the gap effect correction, the scaling correction and the correction for the difference in air attenuation are plotted. The photon beam indices of the beam models used for the calculation of the correction factors reaches from $TPR_{20,10} = 0.599$ (4 MV) up to $TPR_{20,10} = 0.790$ (25 MV).

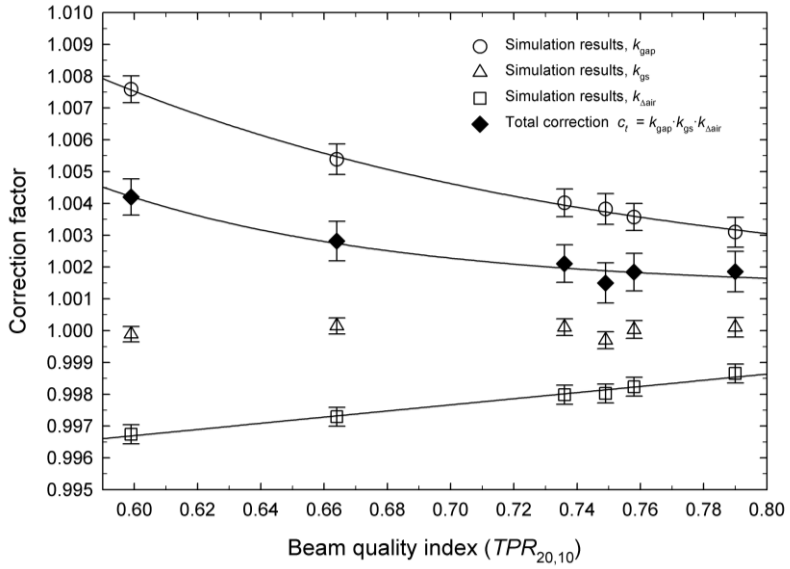

Figure 1: Graphite calorimeter correction factors for high-energy photon beams as a function of $TPR_{20,10}$.

For the gap effect the largest correction was found for the 4 MV photon beam. The corrections magnitude decreases with increasing $TPR_{20,10}$ according to the energy dependence reported by [22],[24]. The exponential function used to fit the simulation data in the mentioned range indicates that the correction factors converge to a value of about 1.003.

For the scaling correction the simulation results were found to be very close to unity and no significant dependence on beam quality index can be reported. The corrections magnitude is altering around unity in the range of k_{gs} = 0.9997 to 1.0001. Consequently for the correction the value unity is assumed and further considered within the uncertainty budget.

Corrections for the difference in air attenuation closer to unity were found for the higher beam qualities. This can be explained with the lower amount of attenuation due to the increasing mean energy of the photon beams with increasing beam quality index. The simulation results show a similar dependence to the tabulated mass attenuation coefficients for air which show a quiet linear decrease of the attenuation coefficient for energies in the interval of 1–10 MeV. The mean spectral photon energies of the spectra used for the simulations are between 1 and 6 MeV.

The corrections for the effective measuring depth in the graphite phantom k_{gc} and k_{gi} are determined by depth dose measurements in graphite individually for each beam quality. Therefore it is necessary to interpolate on the depth dose curves to obtain the correction factor for the required measuring depth. This is performed with the use of the graphite calorimeter itself or with a PTW 30012 ionization chamber by placing additional graphite plates to the graphite phantom.

To obtain graphite calorimeter corrections for different medical high-energy photon beams dependent on beam quality the following types of regression functions are introduced, see figure 1. For the effect of the gaps a three-parameter exponential fit is used based on the relation $k_{gap} = y_0 + a \cdot \exp(-b \cdot TPR_{20,10})$. A linear fit was considered appropriate within the concerned range of beam quality for the air attenuation correction, according to $k_{\Delta air} = y_0 + a \cdot TPR_{20,10}$. The regression parameters y_0, a and b are stated in table 1. To indicate the general beam quality dependence of the graphite calorimeter correction factors (for a subsequent dose conversion with Method 1) the total graphite calorimeter specific correction factor c_t is used, see figure 1. This correction factor is defined as the product of the simulated correction factors k_{gap}, k_{gs} and $k_{\Delta air}$. For this correction a three-parameter exponential fit according to k_{gap} is used. It can be seen that the overall beam quality dependence expressed by c_t is about 0.3 %. Nevertheless to assign the graphite calorimeter corrections the regression equations for each correction factor are used.

Table 1: Calculated regression parameters for the Monte Carlo simulated graphite calorimeter correction factors.

Correction/Conversion factor	Regression parameter		
	y_0	a	b
correction for the effect of the gaps, k_{gap}	1.0012	0.2498	6.1239
air attenuation correction, $k_{\Delta air}$	0.9909	0.0097	n/a
ratio of the mass-energy absorption coefficients, $(\overline{\mu_{en}}/\rho)_{w,g}$	1.1108	$1.4576 \cdot 10^{-6}$	11.8066
ratio of the absorbed dose to collision kerma, $\beta_{w,g}$	1.0001	$1.0782 \cdot 10^{-6}$	9.5064

Since the measurement conditions for ^{60}Co and high-energy photon beams are different it should be mentioned that the introduced regression functions do not provide the correction factors for ^{60}Co gamma ray beams. Those corrections were considered separately.
The chamber perturbation correction factors in water $p_{Q,w}$ and graphite $p_{Q,g}$ defined as product of $p_{wall} \cdot p_{cav} \cdot p_{dis} \cdot p_{cel}$ are evaluated as follows: The wall correction factor p_{wall} which accounts for the difference of the chamber wall material to the surrounding phantom medium is taken as unity for measurements in graphite. For the measurements in water the correction p_{wall} was taken from [25]. The fluence correction factor p_{cav} is assumed to be unity as declared by [25],[26]. The displacement correction factor p_{dis} for measurements in water is calculated according to [26]. In graphite, p_{dis} was obtained by considering the mean graphite density (1.755 g cm^{-3}) occurring by the ionization chamber measurements in the graphite phantom. The correction factor for the central electrode p_{cel} is assumed to be equal for the measurements in the graphite- and the water phantom.

3.2. Beam quality specific absorbed dose conversion factors

The values for the ratios of $(\overline{\mu_{en}}/\rho)_{w,g}$ and $\beta_{w,g}$ of water and graphite were taken from [14],[24],[27],[28]. Since it is intended to use the graphite calorimeter at different accelerators the results of all these studies (considering a multitude of photon beams for their evaluation) were considered. To evaluate $(\overline{\mu_{en}}/\rho)_{w,g}$ and $\beta_{w,g}$ in dependence of beam quality, in terms of $TPR_{20,10}$, the following three-parameter exponential functions are used: $(\overline{\mu_{en}}/\rho)_{w,g} = y_0 + a \cdot \exp(b \cdot TPR_{20,10})$ and $\beta_{w,g} = y_0 + a \cdot \exp(b \cdot TPR_{20,10})$. Figure 2 shows the applied ratios of $(\overline{\mu_{en}}/\rho)_{w,g}$ and β_{wg} as function of $TPR_{20,10}$. The applied regression parameters are declared in table 1. The restricted collision mass stopping power ratios $s_{w,air}$ and $s_{g,air}$ are calculated with use of the third degree polynomials given in [17].

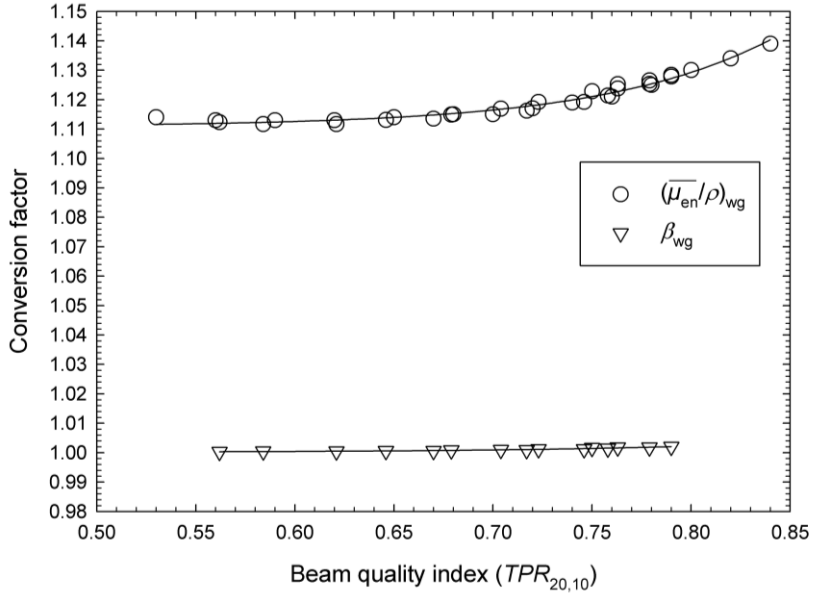

Figure 2: Ratios of the average mass-energy absorption coefficients $(\overline{\mu_{en}}/\rho)_{w,g}$ and of the absorbed dose to collision kerma β_{wg} as a function of $TPR_{20,10}$ required for the absorbed dose conversion.

3.3. Uncertainty budget

The uncertainty budget of the graphite calorimeter for the determination of absorbed dose in high-energy photon beams is presented in table 2. Within this paper only the new evaluated correction and conversion factors are discussed, since the other contributors to the overall uncertainty are described in [1],[2]. The uncertainties in table 2 refer to a quasi-adiabatic absorbed dose to graphite measurement and to a conversion into absorbed dose to water with both methods.

Table 2: Graphite calorimeter uncertainty budget for the realization of the unit of absorbed dose to water at high-energy photon beams.

Quantity	**Uncertainty (%)**	
Quasi-adiabatic determination of D_g	Type A	Type B
core mass, m_c	0	0.12
correction factor for quasi-adiabatic operation, K_{ad}	0.05	0
quasi-adiabatic calibration factor, k_1	0.02	0.15
correction for the effect of the gaps, k_{gap}	0	0.15
interpolation on depth dose curve, k_{gc}	0	0.03
correction for the beam non-uniformity k_{bu}	0	0.10
irradiation time t (used within the evaluation program)	0	0.03
Combined relative standard uncertainty in D_g	**0.272**	

Conversion to absorbed dose to water D_w	**Method 1: by calculation**		**Method 2: with ionization chamber**	
	Type A	Type B	Type A	Type B
distance source to graphite / water phantom $(R_g/R_w)^2$ (virtual point source position)	0	0.30	–	–
ratio of the mass-energy absorption coefficients, $(\overline{\mu_{en}}/\rho)_{w,g}$	0	0.28	–	–
ratio of the absorbed dose to collision kerma, $\beta_{w,g}$	0	0.10	–	–
air attenuation correction, $k_{\Delta air}$	0	0.03	–	–
scaling correction, k_{gs}	0	0.04	–	–
depths / chamber position in graphite and in water, k_{depth}	0	0.10	0	0.07
front wall of water phantom, k_{front}	0	0.05	0	0.05
bremsstrahlung and annihilation radiation correction k_{bs}	0	0.10	–	–
pair production correction k_{pp}	0	0.05	–	–
measurement of collected charge ratio, Q_w/Q_g	–	–	0.05	0.05
ratio of restricted collision mass stopping power $s_{w,air}/s_{g,air}$	–	–	0	0.28
ratio of chamber perturbation correction factors $p_{Q,w}/p_{Q,g}$	–	–	0	0.32
interpolation on depth dose curve, k_{gi}	–	–	0	0.03
Combined relative standard uncertainty for conversion	**0.456**		**0.442**	
Combined relative standard uncertainty in D_w **method 1**	**0.53**			
Combined relative standard uncertainty in D_w **method 2**	**0.52**			

For the estimation of the correction factors uncertainties the simulations statistical uncertainties, the uncertainties in the Monte Carlo geometry models, the uncertainties of the applied regression functions and the uncertainty for the determination of $TPR_{20,10}$, both within the measurement and within the simulation are taken into account. The applied regression functions for the effect of gap and for the air attenuation fit the simulation results better than 0.01 %.

Based upon the results of the investigations in [15],[16] the uncertainty for an estimation of the virtual point source position is considered within the uncertainty budget. It should be mentioned that these estimates lead to significant larger uncertainties than to a detailed determination based upon a combination of experimental and Monte Carlo methods, see [14]. Further should be mentioned that if an external monitor chamber is used for the measurements a backscatter correction is necessary, in

particular for application of dose conversion according to Method 1. Since the graphite phantom is placed only a few centimeter in front of the monitor chamber.
The uncertainties of the physical constants ($(\overline{\mu_{en}/\rho})_{w,g}$, $\beta_{w,g}$, $s_{w,air}/s_{g,air}$) used for the absorbed dose conversion are a combination of the published uncertainties of the values and the uncertainty of the implemented fit for the determination of the beam quality specific conversion factors. The introduced regression functions allow to fit the data of $(\overline{\mu_{en}/\rho})_{w,g}$ with uncertainties of about 0.2 % and respectively $\beta_{w,g}$ with 0.02 %.
For the uncertainty of the ratio $p_{Q,w}/p_{Q,g}$ the uncertainties of $p_{cav}{\cdot}p_{dis}$ for measurements in graphite and water, derived from the corresponding literature [26], were taken into account Thereby the stated systematic uncertainty and the uncertainty of the applied empirical formula is considered. Further the uncertainty of p_{wall} as stated in [25] is included.
The overall uncertainty for the determination of absorbed dose to water (table 2) with the BEV graphite calorimeter at high-energy photon beams is larger than the uncertainties reported in [3] which are in the order of 0.4 % - 0.5 %.

4. Verification

A verification of the graphite calorimeter development and respectively of the implemented correction and conversion factors for high-energy photon beams was done in the framework of the EURAMET project 1021 (see [7]) - intended for the direct comparison of absorbed dose primary standards in ^{60}Co and high-energy photon beams, see figure 3. The participating NMI's were: BEV, Swiss Federal Office of Metrology (METAS) and the German Physikalisch-Technische Bundesanstalt (PTB). For the comparison exercise the BEV transported the graphite calorimeter primary standardization system to METAS and PTB for operation in the accelerator radiation fields. The measurements were carried out in ^{60}Co and high-energy photon beams generated by electrons with energies of 4 MeV, 6 MeV, 10 MeV and 15 MeV.

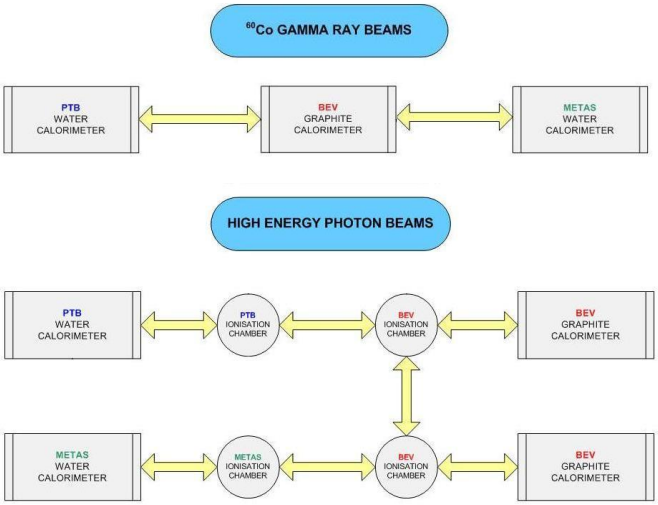

Figure 3: Concept of the comparison excercise EURAMET project 1021

The results of project part regarding ^{60}Co are published in [4].
This was the first time that an absorbed dose primary standard calorimeter of one NMI was transported to a different NMI for the purpose of a direct comparison in accelerator high-energy photon beams. The project was connected with a huge logistic effort (transportation and setup of the calorimeter system including graphite phantom, measurement– and evaluation device, vacuum pump, ionization chamber measurement system etc.) and with a lot of expected and unexpected challenges.
The Measurements in high-energy photon beams were carried out in three steps:

- Determination of absorbed dose to water at the accelerator at PTB, respectively METAS and calibration of an ionization chamber.
- Calibration of the same ionization chamber PTW 30012-27 using an ionization chamber of PTB respectively METAS, calibrated with the water calorimeter of PTB respectively METAS.

- Comparison of the calibration coefficients.

The BEV graphite calorimeter was used in the quasi-adiabatic operation mode to obtain the absorbed dose to graphite. The conversion to absorbed dose to water was done with method 2. The use of the method 1 for accelerator measurements is affected by two problems which could not be solved in the short time:

- The effective (virtual) point of source of an accelerator beam must be well known
- Backscatter influences to the monitor chamber from the graphite phantom as a result of the small distance according to the photon fluence scaling theorem must be considered

At the METAS accelerator deviations between 0.3 % and 0.7 % for the four energies were obtained. The results for the PTB accelerators are problematical. Deviations between 1.5 % and 2.2 % were achieved. The reason for the discrepancy seems to be clear. The measurements with the ionization chamber in the graphite phantom were made immediately after the graphite calorimeter measurements with a working temperature of 27 °C. Therefore a temperature effect – which influences the ionization current measurement – is assumed. Considering these circumstances one obtains a shift in the right direction. Unfortunately a retrospective correction is not possible.

Nevertheless, and especially under consideration of the very short measuring time at PTB, respectively at METAS the project was very successful. Only five days were scheduled and necessary for five energies including setups of the graphite calorimeter and calibration of the ionization chambers and of course solving of some of the unexpected problems. The mobile application of the BEV graphite calorimeter was shown impressively. Within a very short time very satisfactory results can be obtained. The results obtained by the different NMI's are widely in agreement.

Comparing the ionization chamber calibration coefficients of PTB and METAS for the four considered high-energy photon beam qualities deviations between 0.2 % and 0.9 % were obtained.

It has to be noted that the experimental re-determination of the correction factors k_Q at the new PTB-accelerators wasn't finished at time of the comparison. Therefore the PTB-BEV-comparison was carried out with a chamber of the PTB (IBA FC65G-1108) calibrated at ^{60}Co and the factors k_Q given by DIN 6800-2 [29]. Later measurements to realize D_w at 6 MV and 10 MV at PTB are showing a little shift.

5. Conclusions

The working range of the graphite calorimeter for high-energy photon beams reaches from approximately $TPR_{20,10} = 0.59$ to about 0.80, see figure 1. Within this range the correction for the effect of the gaps shows the strongest beam quality dependence of about 0.5 % respectively the correction for the difference in air attenuation about 0.2 %. No significant dependence on beam quality was found for the scaling correction. The overall dependence of the correction factors on beam quality and energy spectrum is small in comparison with the graphite calorimeter application range. That implies that the correction factors calculated with the photon energy spectra of the Varian Linacs and the 25 MV spectrum of the Elekta SL25 accelerator (taken representative for typical medical accelerators beams) constitute irradiation facility independent but beam quality index specific regressions functions. A further consideration of simulation results is intended and could be used to improve the accuracy of the implemented regression functions. The implemented regression functions for the evaluation of correction factors and physical constants in dependence on beam quality index allow using the graphite calorimeter at different accelerators beams. However with significant larger uncertainties especially in the conversion factors in comparison to other NMI's which particularly consider the beam characteristics of a special accelerator.

The carried out works provide the methodic basics to enable the BEV for the accomplishment of primary standard dosimetry of various high-energy photon beams. Accordingly secondary standard ionization chamber calibrations in terms of absorbed dose to water at high-energy photon beams can be performed.

A confirmation of the energy range and application enhancement of the graphite calorimeter and thus of the implemented correction and conversion factors was done in the framework of the EURAMET project 1021. The participation on the comparison exercise further demonstrates the feasibility on principle of transporting the graphite calorimeter and providing calibrations of ionization chambers at various accelerators - however it is connected with a big logistic effort.

The improvement of the primary standard directly leads to an improvement of quality assurance measurements in Linac radiotherapy, i.e. directly related to the radiation protection of patient. Since the accurate knowledge of the applied dose is a main factor influencing the success of a radiotherapy and therefore of great importance for the treatment planning.

Acknowledgements

The accomplishment of the BEV high-energy absorbed dose graphite calorimetry project was promoted by the Physico-technical Testing Service (PTP), which is a partial legal entity of BEV.
The authors wish to thank Dr. Josef Witzani for his encouragement and for his valuable comments, along with many thanks to all colleagues of the dosimetry laboratory for their support.
The authors are grateful to Prim. Univ.-Doz. Dr. Brigitte Pakisch from the hospital Wiener Neustadt for giving them the opportunity of collaboration and to DI Michael Vejda for his support at the Varian Clinac accelerators.
The authors thank Dr. Ralf-Peter Kapsch (PTB) and Dr. Gerhard Stucki (METAS) for the excellent cooperation in the framework of the EURAMET project 1021

References

[1] Leitner A and Witzani J 1995 The Realization of the Unit of Absorbed Dose at the Austrian Dosimetry Laboratory Seibersdorf, Internal report OEFZS-4740.
[2] Witzani J, Duftschmid K E, Strachotinsky Ch and Leitner A 1984 A Graphite Absorbed-Dose Calorimeter in the Quasi-Isothermal Mode of Operation, Metrologia 20 73-79.
[3] Seuntjens J and Duane S 2009 Photon absorbed dose standards, Metrologia 46 S39-S58.
[4] Baumgartner A, Steurer A, Maringer F-J, Tiefenboeck W, Gabris F, Kapsch R-P, Stucki G 2011 "Correction factors of an absorbed dose primary standard graphite calorimeter in ^{60}Co gamma ray beams" Radiation Protection Dosimetry (2011) 145(1): 3-12.
[5] Kessler C, Allisy-Roberts P. J, Steurer A, Baumgartner A, Tiefenboeck W and Gabris F 2010 Comparison of the standards for absorbed dose to water of the BEV, Austria, and the BIPM for ^{60}Co gamma radiation. Metrologia 47 (Tech. Suppl. 06017)
[6] Baumgartner A (2010) "Primary standard dosimetry of high-energy photon and electron beams" Ph.D. Thesis in German language (Vienna University of Technology).
[7] Steurer A, Baumgartner A, Kapsch R-P, Stuck G, Maringer F-J (2011) "EURAMET TC-IR Project 1021 - Direct comparison of primary standards of absorbed dose to water in ^{60}Co and high-energy photon beams", Final Report (http://www.euramet.org/index.php?id=tc-ir-projects).
[8] Andreo P, Burns D T, Hohlfeld K, Huq M S, Kanai T, Laitano F, Smyth V G, Vynckier S 2000 Absorbed dose determination in external beam radiotherapy: an international code of practice for dosimetry based on standards of absorbed dose to water. TRS-398, IAEA Vienna.
[9] ICRU REPORT No 64 2001 Dosimetry of High-Energy Photon Beams Based on Standards of Absorbed Dose to Water, International Commission on Radiation Units and Measurements.
[10] ICRU REPORT No 60 1998 Fundamental Quantities and Units for Ionizing Radiation, International Commission on Radiation Units and Measurements.
[11] ÖNORM S 5234-3 2009 Clinical dosimetry - Part 3: Ionization chamber dosimetry in teletherapy (Austrian standard, in German), Austrian Standards Institute.
[12] Pruitt J S and Loevinger R 1982 The photon-fluence scaling theorem for Compton-scattered radiation, Med Phys 9, 176-179.
[13] McEwen M R and Duane S 2000 Development of A Portable Graphite Calorimeter for Photons and Electrons, Proceedings of NPL Workshop on Recent Advances in Calorimetric, Absorbed Dose Standards. Workshop held December 8 - 10 1999
[14] Nutbrown R F, Duane S, Shipley D R and Thomas R A S, 2002 Evaluation of factors to convert absorbed dose calibrations from graphite to water for the NPL high-energy photon calibration service, Phys. Med. Biol. 47.
[15] Tatcher M and Bjärngard B 1992 Head-scatter factors and effective x-ray source positions in a 25-MV linear accelerator, Med Phys. 19(3): 685-6.

[16] McKenzie A L and Stevens P H 1993 How is photon head scatter in a linear accelerator related to the concept of a virtual source?, Phys Med. Biol. 38 1173-1180.
[17] Andreo P 1994 Improved calculations of stopping power ratios and their correlation with the quality of therapeutic photon beams. Measurement Assurance in Dosimetry, proceedings of a symposium 335-359, IAEA Vienna.
[18] Salvat F, Fernández-Varea J.M and Sempau J. 2006 PENELOPE-2006: A Code System for Monte Carlo Simulation of Electron and Photon Transport. OECD Nuclear Energy Agency, Issy-les-Moulineaux, France.
[19] Baumgartner A, Steurer A and Maringer F J 2009 Simulation of photon energy spectra from Varian 2100C and 2300C/D Linacs: Simplified estimates with PENELOPE Monte Carlo models, Applied Radiation and Isotopes 67, 2007–2012.
[20] Sheikh-Bagheri D and Rogers D W O 2002 Monte Carlo calculation of nine megavoltage photon beam spectra using the BEAM code, Med. Phys. 29(3) 391-402.
[21] Boutillon M 1989 Gap correction for the calorimetric measurement of absorbed dose in graphite with a ^{60}Co beam, Phys. Med. Biol. 34, 1809–1821.
[22] Owen B and DuSautoy A R 1991 Correction for the effect of the gaps around the core of an absorbed dose graphite calorimeter in high energy photon radiation, Phys. Med. Biol. 36, 1699-1704.
[23] Hubbell J H and Seltzer S M Tables of X-Ray Mass Attenuation Coefficients and Mass Energy-Absorption Coefficients from 1 keV to 20 MeV for Elements Z = 1 to 92 and 48 Additional Substances of Dosimetric Interest*, Ionizing Radiation Division, Physics Laboratory National Institute of Standards and Technology Gaithersburg, MD 20899.
[24] Wise K N 2001 Monte Carlo Methods used to develop the Australian Absorbed Dose Standard. Australian Radiation protection and Nuclear safety Agency, Technical Report 132.
[25] Wulff J, Heverhagen J T and Zink K, 2008 Monte-Carlo-based perturbation and beam quality correction factors for thimble ionization chambers in high-energy photon beams, Phys. Med. Biol. 53 2823–2836.
[26] Wang L L W and Rogers D W O 2009 The replacement correction factors for cylindrical chambers in high-energy photon beams, Phys. Med. Biol. 54 1609–1620.
[27] Andreo P, Cunningham J R and Hohlfeld K, 1987 Absorbed dose determination in photon and electron beams: an international code of practice. TRS-277, IAEA Vienna.
[28] Domen S R and Lamperti J P 1974 A Heat-loss Compensated Calorimeter: Theory Design and Performance, J. Res. Nat. Bur. Stand. 78A, 595-610.
[29] DIN 6800-2 2008 "Dosismessverfahren nach der Sondenmethode für Photonen- und Elektronenstrahlung – Teil 2: Dosimetrie hochenergetischer Photonen- und Elektronenstrahlung mit lonisationskammern". (German standard, in German)